Supplementary information

Electronic modification of $NaCrO_2$ *via* Ni^{2+} substitution as efficient cathode for sodium-ion batteries

Jingyao Cai[1], Yanbing Zhu[1], Zhiguo Zhang[1], Jiandong Zhang[1], Liyuan Tian[2], Pengkun Gao[3], Yali Zhang[3], Mingkui Wang[1,2], Yan Shen[1,*]

[1]Wuhan National Laboratory for Optoelectronics, Huazhong University of Science and Technology, Wuhan 430074, Hubei, China.
[2]China-EU Institute for Clean and Renewable Energy, Huazhong University of Science and Technology, Wuhan 430074, Hubei, China.
[3]PYTES (Shandong) Energy Technology Co. Ltd., Building 1, High-Tech Industrial Park, Weishan County, Jining 272000, Shandong, China.

***Correspondence to:** Prof. Yan Shen, Wuhan National Laboratory for Optoelectronics, Huazhong University of Science and Technology, Luoyu Road 1037, Wuhan 430074, Hubei, China. E-mail: ciac_sheny@mail.hust.edu.cn

1. Experimental section

1.1 Material characterization

The crystallographic properties of samples and ex-situ XRD measurements were analyzed by X-ray powder diffraction (Empyrean) with Cu Kα radiation (λ=1.5406 Å) from 5° to 90°. For the ex-situ XRD experiment, cells were charged at 0.2 C for different cycles, and then disassembled. The $NaCr_xNi_{1-x}O_2$ electrodes were rinsed with dimethyl carbonate (DMC) in the glove box before the XRD experiment. The morphology and size of the samples were determined by a scanning electron microscope (SEM, Nova Nano SEM 450). Transmission electron microscopy (TEM, Tecnai G2 F30 S-TWIN) and were performed to study the microstructures of the samples. The elemental ratio is confirmed by inductively coupled plasma spectroscopy (ICP, Agilent ICPOES730). The degree of oxidation in the synthesized samples was studied by X-ray photoelectron spectroscopy (XPS, Thermo ESCALAB 250Xi).

1.2 Electrochemical characterization

The working electrode or the cathode was prepared by mixing the active material (80%), Super P (10%), and polyvinylidene fluoride (PVDF) in N-methyl-pyrrolidone (NMP) (10%) solvent to form a uniform slurry. This slurry was then coated onto a carbon-covered aluminum foil and vacuum dried at 120 °C for 12 h to eliminate residual moisture. Electrochemical properties tests were carried out with CR2023 coin half-cells comprised of the $NaCr_xNi_{1-x}O_2$ cathode and a sodium metal anode with 1 M $NaPF_6$ in EC: DMC=1:1 Vol% and glass-fiber separators (GF/D). The active mass loading was 2.3–2.7 mg cm^2. Electrochemical performance tests were conducted at 25 °C using a Land BTI-10 battery testing system. Galvanostatic cycling was carried out between 2.0 and 3.6 V. An electrochemical working station (CHI 660D model) was employed to carry out cyclic voltammetry experiments at a scanning rate of 0.1 mV s^{-1} between 2.0 and 3.6 V.

The galvanostatic intermittent titration technique test was performed to investigate the diffusion coefficient of materials. The batteries were charged at a current density of 20 mA g^{-1} for 15 minutes, followed by open circuit relaxation for 1 hour. The detailed calculation is shown as follows:

$$D_{Na^+} = \frac{4}{\pi\tau}\left(\frac{mV_m}{MA}\right)^2\left(\frac{\Delta E_s}{\Delta E_\tau}\right)^2$$

where m and M are the mass and molecular weight, τ are duration of the current pulse, V_m is the molar volume, A is the contact surface area between the electrode and electrolyte, ΔE_s and ΔE_τ are the change in steady-state voltages after a current pulse and voltage change during a current pulse.

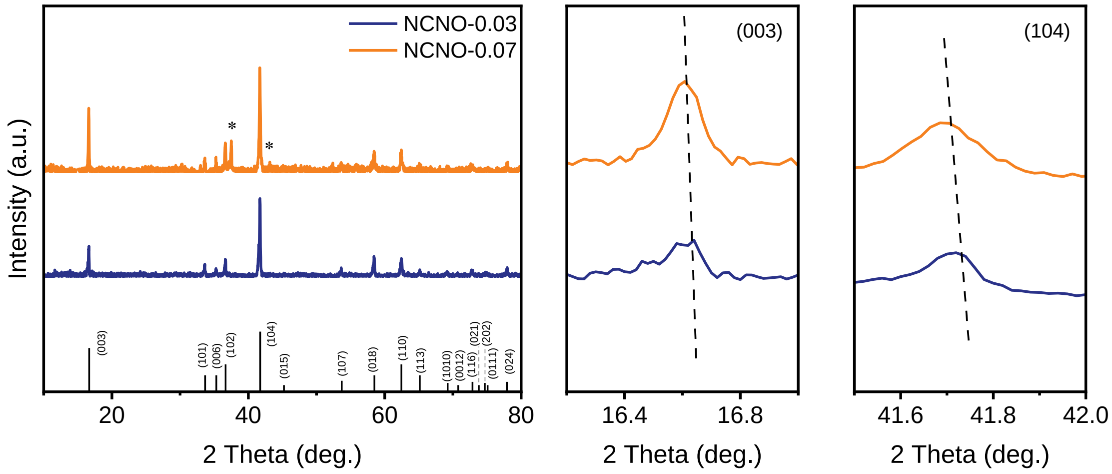

Supplementary Figure 1. XRD patterns of synthesized samples and the magnified diffraction peaks for the (003) and the (104) planes.

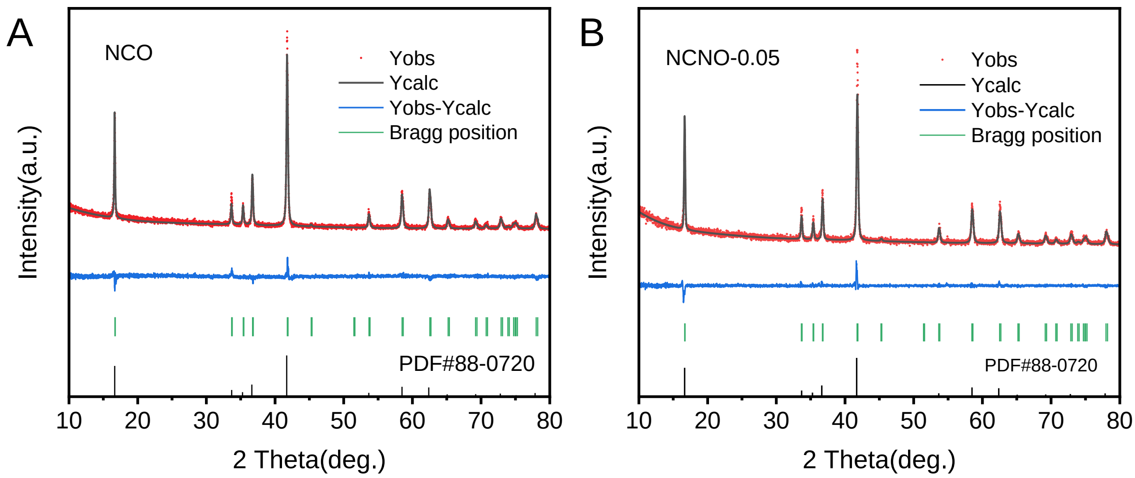

Supplementary Figure 2. Rietveld refinement for XRD patterns of (A) the NCO and (B) the NCNO-0.05 samples, including those for experimental observation and theoretical calculation as well as the difference between them to indicate the reliability factors. The XRD patterns of $NaCrO_2$ can be referred to JCPDS Card No. 88-0720.

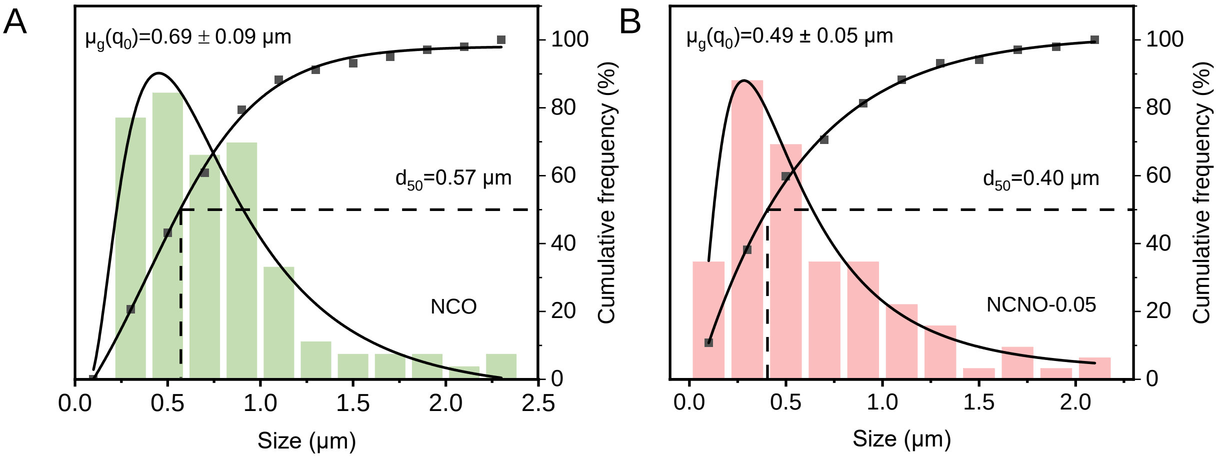

Supplementary Figure 3. Particles size distribution of (A) NCO and (B) NCNO-0.05.

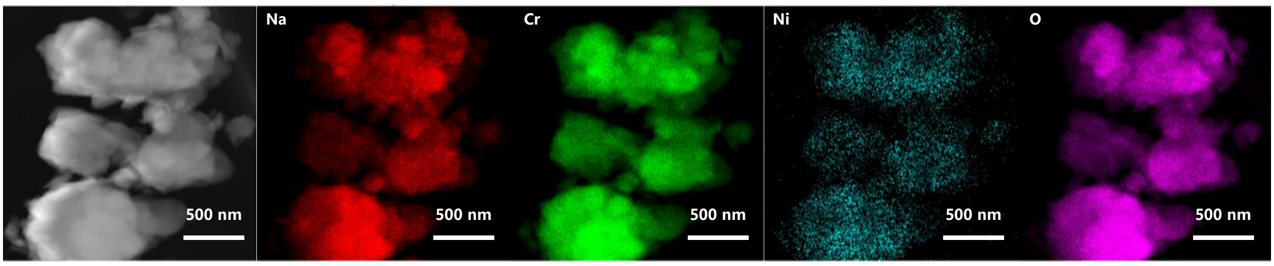

Supplementary Figure 4. STEM image and the energy dispersive spectroscopy mapping images of the layered NCNO-0.05 sample.

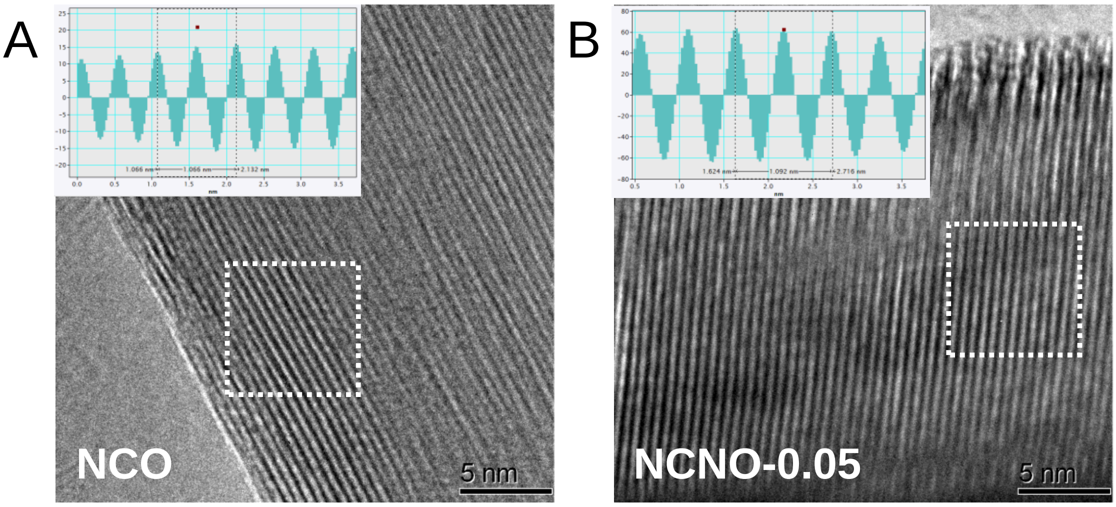

Supplementary Figure 5. HRTEM images for (A) NCO and (B) NCNO-0.05.

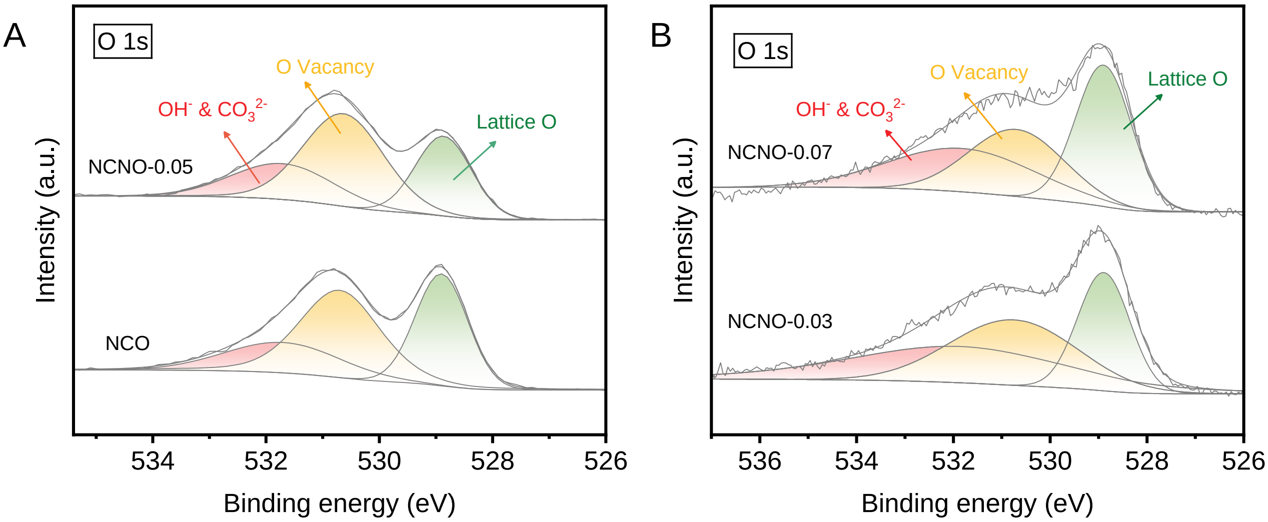

Supplementary Figure 6. The XPS spectra of O 1s in samples.

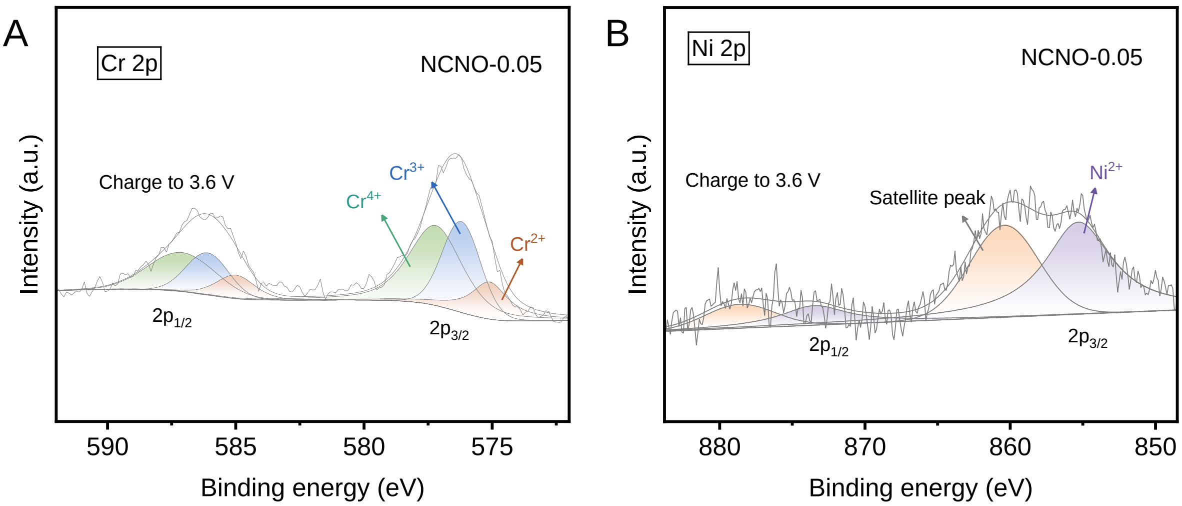

Supplementary Figure 7. The ex-situ XPS spectra of NCNO-0.05 when charged to 3.6 V (vs. Na^+/Na) (A) Cr 2p (B) Ni 2p.

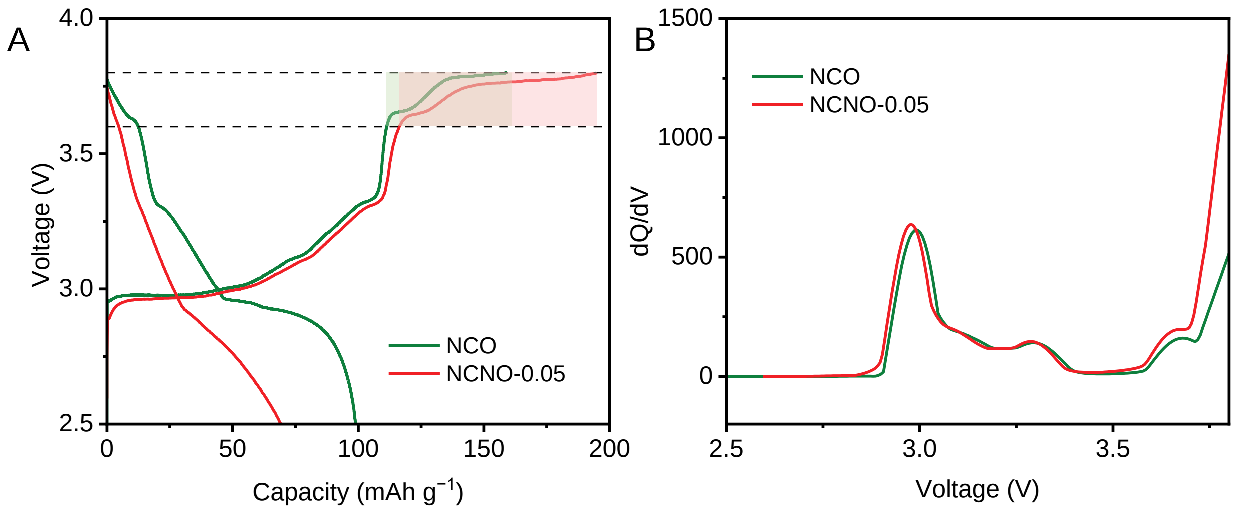

Supplementary Figure 8. (A) The charge curves of the NCO and NCNO-0.05 samples. (B) The capacity differential curves of NCO and NCNO-0.05.

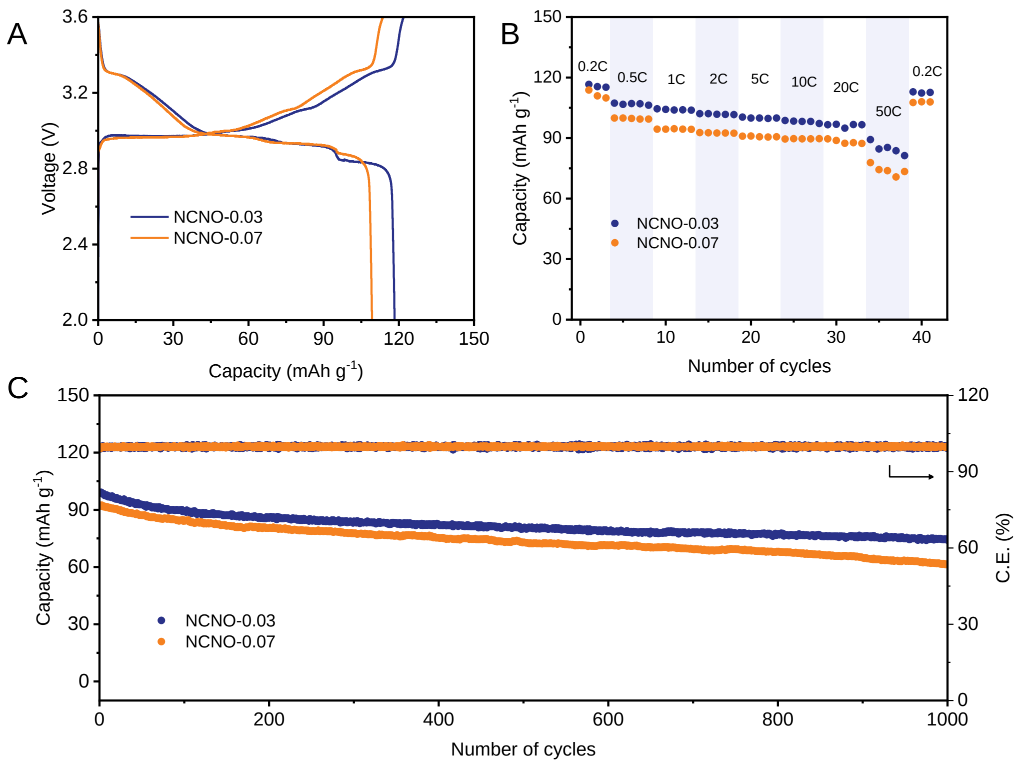

Supplementary Figure 9. (A) The charge/discharge profiles of CR2032 type coin cells assembled with the prepared the NCNO-0.03 and NCNO-0.07 samples as the working electrode and Na foils as the counter electrode. The discharge rate is 0.2 C. (B) The rate behaviors of CR2032 type coin cells. (C) The cycling performances of CR2032 type coin cells at a rate of 10 C.

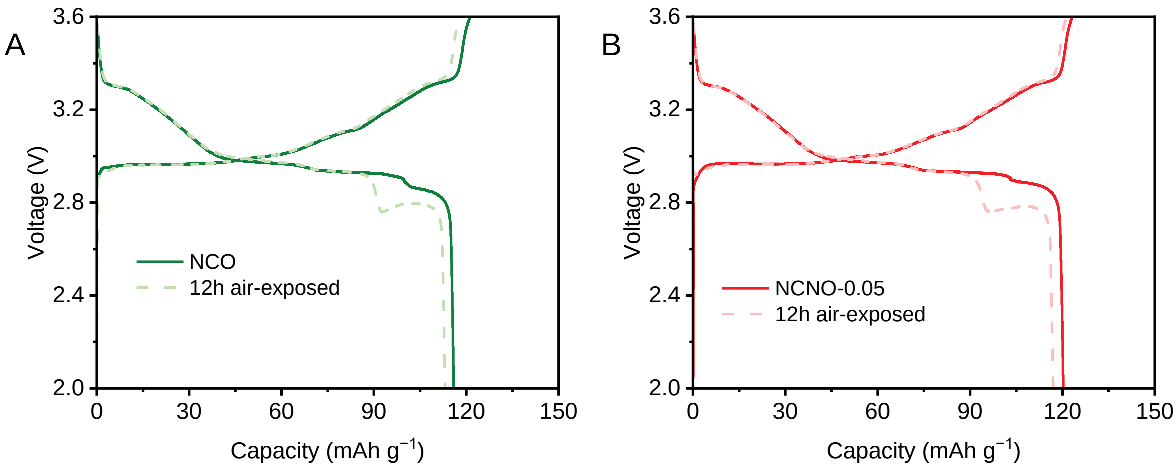

Supplementary Figure 10. The air stability of the NCO and NCNO-0.05 samples.

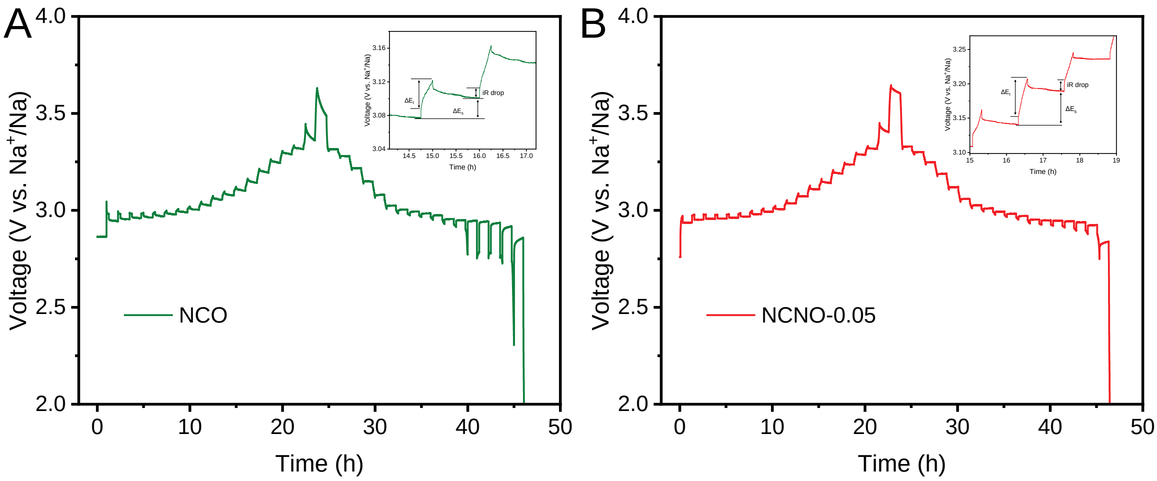

Supplementary Figure 11. GITT curves in (A) NCO and (B) NCNO-0.05 at the initial charging-discharging process and a partially enlarged version of the GITT profile (the inset).

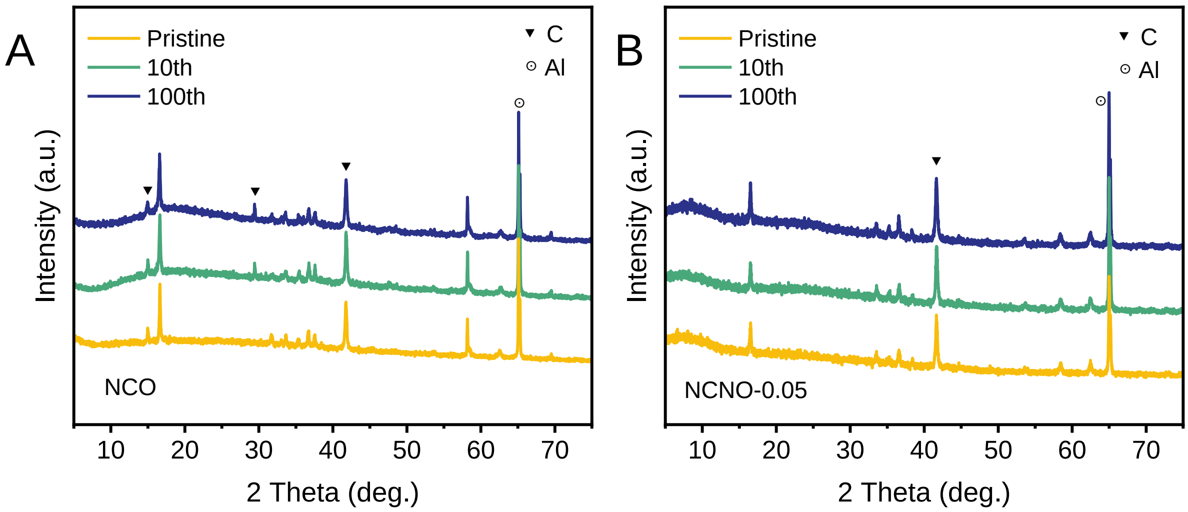

Supplementary Figure 12. XRD patterns of the (A) NCO and (B) NCNO after different cycles.

Table S1. Rietveld refinement results of the XRD data of (a) NCO, and (b) NCNO-0.05 powders.

(a)

Phase	NCO	
Space Group	R-3m	
Cell parameters	a (Å)	2.9697
	b (Å)	2.9697
	c (Å)	15.9746
	α (°)	90.0000
	β (°)	90.0000
	γ (°)	120.0000
Agreement ractors	R_{wp}(%)	9.1100
	R_p(%)	6.6400
	χ^2	1.9800

(b)

Phase	NCNO-0.05	
Space Group	R-3m	
Cell parameters	a (Å)	2.9737
	b (Å)	2.9737
	c (Å)	15.9966
	α (°)	90.0000
	β (°)	90.0000
	γ (°)	120.0000
Agreement ractors	R_{wp}(%)	8.4600
	R_p(%)	6.7700
	χ^2	1.7070

Table S2. EDS results of NCNO-0.05

Atomic ratio measured by EDS analysis		
	Cr	Ni
NCNO-0.05	0.952	0.047

Table S3. ICP analyses of atomic ratio of Na, Cr and O NCNO-0.05 with standard deviation

Atomic ratio measured by the Inductively Coupled Plasma			
	Na	Cr	Ni
NCNO-0.05	1	0.946	0.048

Table S4. Comparison of electrochemical properties of $NaCrO_2$ substituted by different elements.

Materials	Voltage range（V）	Best rate capability（mAh g^{-1}）	Best cyclying	Ref
$Na_{0.72}Cr_{0.86}Sb_{0.14}O_2$	1.5 - 4.1	~125 at 5C	78.64% after 200 cycles at 2 C	[1]
$NaCr_{0.95}Ni_{0.05}O_2$	2.0 - 3.6	91.2 at 50C	80% after 1000 cycles at 10C	This work
$Na_{0.88}Cr_{0.88}Ru_{0.12}O_2$	1.5 - 3.8	83.6 at 50C	80.7% after 1100 at 10C	[2]
$Na_{0.9}Ca_{0.035}Cr_{0.97}Ti_{0.97}O_2$	1.5 - 3.8	51.6 at 100C	81% after 1000 cycles at 10C	[3]
$Na_{0.9}Cr_{0.95}Sb_{0.05}O_2$	2.5 -3.5	96.1 at 32C	70.9% after 1000 cycles at 5 C	[4]
$Na_{0.9}Ca_{0.05}CrO_2$	2.0 – 3.6	50 at 20C	76% after 500 cycles at 0.2C	[5]
$NaCr_{0.8}Mn_{0.2}O_2$	2.0 – 3.8	68 at 2C	86% after 200 cycles at 0.2C	[6]

References

1. Ko W, Cho MK, Kang J, et al. Exceptionally increased reversible capacity of O3-type $NaCrO_2$ cathode by preventing irreversible phase transition. *Energy Storage Mater* 2022;46:289-99. **DOI:** **10.1016/j.ensm.2022.01.023**
2. Xi K, Chu S, Zhang X, et al. A high-performance layered Cr-Based cathode for sodium-ion batteries. *Nano Energy* 2020;67:104215. **DOI:** **10.1016/j.nanoen.2019.104215**
3. Lee I, Oh G, Lee S, et al. Cationic and transition metal co-substitution strategy of O3-type $NaCrO_2$ cathode for high-energy sodium-ion batteries. *Energy Storage Mater* 2021;41:183-95. **DOI:** **10.1016/j.ensm.2021.05.046**
4. Ma C, Li XL, Yue XY, et al. Suppressing O3−O’3 phase transition in $NaCrO_2$ cathode enabling high rate capability for sodium-ion batteries by Sb substitution. *Chem Eng J* 2022;432:134305. **DOI:** **10.1016/j.cej.2021.134305**

5. Zheng L, Bennett J, Obrovac M, et al. Stabilizing $NaCrO_2$ by Sodium Site Doping with Calcium. *J Electrochem Soc* 2019;166:A2058. **DOI:** **10.1149/2.1041910jes**

6. Y. Wang, P. Cui, W. Zhu, Z. Feng, M. Vigeant, H. Demers, A. Guerfi, K. Zaghib, Enhancing the electrochemical performance of an O3–$NaCrO_2$ cathode in sodium-ion batteries by cation substitution. *J Power Sources* 2019;43:226760. **DOI:** **10.1016/j.jpowsour.2019.226760**